

Supplemental material: Retrieving time-dependent Green's functions in optics with low-coherence interferometry

Amaury Badon, Geoffroy Lerosey, Albert C. Boccara, Mathias Fink, and Alexandre Aubry*
ESPCI ParisTech, PSL Research University, CNRS, Institut Langevin, UMR 7587, 1 rue Jussieu, F-75005 Paris, France

(Dated: January 12, 2015)

TIME-REVERSAL AND MUTUAL COHERENCE FUNCTION OF A RANDOM WAVE-FIELD

This section provides a theoretical proof for the emergence of the Green's function from the mutual coherence function of an incoherent wave-field, in agreement with the less intuitive theory for Green's function retrieval proposed by Wapenaar and colleagues [1]. The argument is based on fundamental symmetries of reciprocity, time-reversal (TR) invariance and diffraction theory. Indeed, as we will see, there exists a strong analogy between a TR experiment [see Fig.S1] and the mutual coherence function of a random wave-field [see Fig.S2] [2, 3]. Both actually yield the difference between the causal and anticausal Green's functions.

Let us consider a linear, nonmagnetic and inhomogeneous medium. As we will see, a TR experiment can be fully described in terms of the electric Green dyadic $\bar{\bar{g}}(\mathbf{r}, \mathbf{r}', t)$ [4]. It connects the electric field $\mathbf{E}(\mathbf{r}, t)$ measured at point \mathbf{r} when a point source emits a Dirac pulse $\delta(t)$ at point \mathbf{r}' . The electric Green dyadic can be written in terms of its frequency components as $\bar{\bar{g}}(\mathbf{r}, \mathbf{r}', t) = \int_{-\infty}^{+\infty} d\omega \bar{\bar{G}}(\mathbf{r}, \mathbf{r}', \omega) e^{-i\omega t}$. In the frequency domain, the Green dyadic obeys the electromagnetic wave equation with a point source term on the right hand side

$$\nabla_r \times \nabla_r \times \bar{\bar{G}}(\mathbf{r}, \mathbf{r}', \omega) - \frac{\omega^2}{c^2} \bar{\bar{\epsilon}}(\mathbf{r}, \omega) \bar{\bar{G}}(\mathbf{r}, \mathbf{r}', \omega) = -\delta(\mathbf{r} - \mathbf{r}') \bar{\bar{\mathbf{I}}} \quad (\text{S1})$$

where the symbol \times stands for the cross product. $\bar{\bar{\epsilon}}$ is the relative permittivity tensor and $\bar{\bar{\mathbf{I}}}$ is the unit dyadic. The Green's formalism is powerful since the Green dyadic connects the electric field $\mathbf{E}(\mathbf{r}, \omega)$ with any source distribution $\mathbf{S}(\mathbf{r}', \omega)$ in a volume Ω , such that

$$\mathbf{E}(\mathbf{r}, \omega) = \int_{\Omega} \bar{\bar{G}}(\mathbf{r}, \mathbf{r}', \omega) \mathbf{S}(\mathbf{r}', \omega) d\Omega \quad (\text{S2})$$

In agreement with the principle of Huygens Fresnel, the Green dyadic also relates the electric field $\mathbf{E}(\mathbf{r})$ in the volume Ω with the electric field $\mathbf{E}(\mathbf{r}_s)$ on the surrounding surface S . This is the equivalent of the Helmholtz-Kirchoff theorem for electromagnetic waves [4, 5],

$$\mathbf{E}(\mathbf{r}, \omega) \cdot \mathbf{V} = \int_S \left[\mathbf{E}(\mathbf{r}_s, \omega) \times \nabla_{\mathbf{r}_s} \times \bar{\bar{G}}(\mathbf{r}, \mathbf{r}_s, \omega) \mathbf{V} - \bar{\bar{G}}(\mathbf{r}, \mathbf{r}_s, \omega) \mathbf{V} \times \nabla_{\mathbf{r}_s} \times \mathbf{E}(\mathbf{r}_s, \omega) \right] \cdot \mathbf{n} dS \quad (\text{S3})$$

where the symbol \cdot stands for the scalar product. \mathbf{V} is an arbitrary constant vector and \mathbf{n} is the normal to the surface S .

A sketch of a TR experiment is displayed in Fig.S1. In a first step [Fig.S1(a)], a point source emits a pulse at position \mathbf{r}_a . The time reversal mirror (TRM) is passive and records the outgoing field over a surface S [see Fig.S1(b)], assumed to be in the far field of both the source and the inhomogeneities of the medium. In the frequency domain, this field can be expressed as,

$$\mathbf{E}(\mathbf{r}_s, \omega) = \bar{\bar{G}}(\mathbf{r}_s, \mathbf{r}_a, \omega) \mathbf{U}(\omega) \quad (\text{S4})$$

The vector $\mathbf{U}(\omega)$ denotes the orientation of the source at frequency ω . In a second step, the TRM back-emits the time-reversed replica of the outgoing field recorded in the direct situation [see Fig.S1(c)]. The time-reversed wave exactly follows the same trajectory as in the first step but in a reversed way. The wave first converges towards the initial source position [see Fig.S1(d)], collapses and is followed by a diverging wave [see Fig.S1(e)]. Thus the time-reversed field observed as a function of time, from any location, shows two wavefronts of opposite sign [see Fig.S1(f)]. Theoretically, the time-reversed wave field \mathbf{E}_{tr} is shown to correspond to the difference between the causal Green dyadic (diverging wave) and the anticausal Green dyadic (converging wave) [4], such that

$$\mathbf{E}_{\text{tr}}(\mathbf{r}, t) = \left[\underbrace{\bar{\bar{g}}(\mathbf{r}, \mathbf{r}_a, t)}_{\text{causal wave}} - \underbrace{\bar{\bar{g}}(\mathbf{r}, \mathbf{r}_a, -t)}_{\text{anticausal wave}} \right] \otimes \mathbf{u}(-t) \quad (\text{S5})$$

in the time domain, or equivalently

$$\begin{aligned} \mathbf{E}_{\text{tr}}(\mathbf{r}, \omega) &= \left[\bar{\bar{G}}(\mathbf{r}, \mathbf{r}_a, \omega) - \bar{\bar{G}}^*(\mathbf{r}, \mathbf{r}_a, \omega) \right] \mathbf{U}^*(\omega) \\ &= 2i \text{Im} \left\{ \bar{\bar{G}}(\mathbf{r}, \mathbf{r}_a, \omega) \right\} \mathbf{U}^*(\omega) \end{aligned} \quad (\text{S6})$$

in the frequency domain.

We now establish the link between TR and correlation of the Green dyadic. The time-reversed wave-field $\mathbf{E}_{\text{tr}}(\mathbf{r}, \omega)$ results from the diffraction of the wave-field emitted by the TRM, $\mathbf{E}(\mathbf{r}_s, \omega) = \mathbf{E}_o^*(\mathbf{r}_s, \omega)$. Mathematically, it can be expressed by injecting Eq.S4 into Eq.S3:

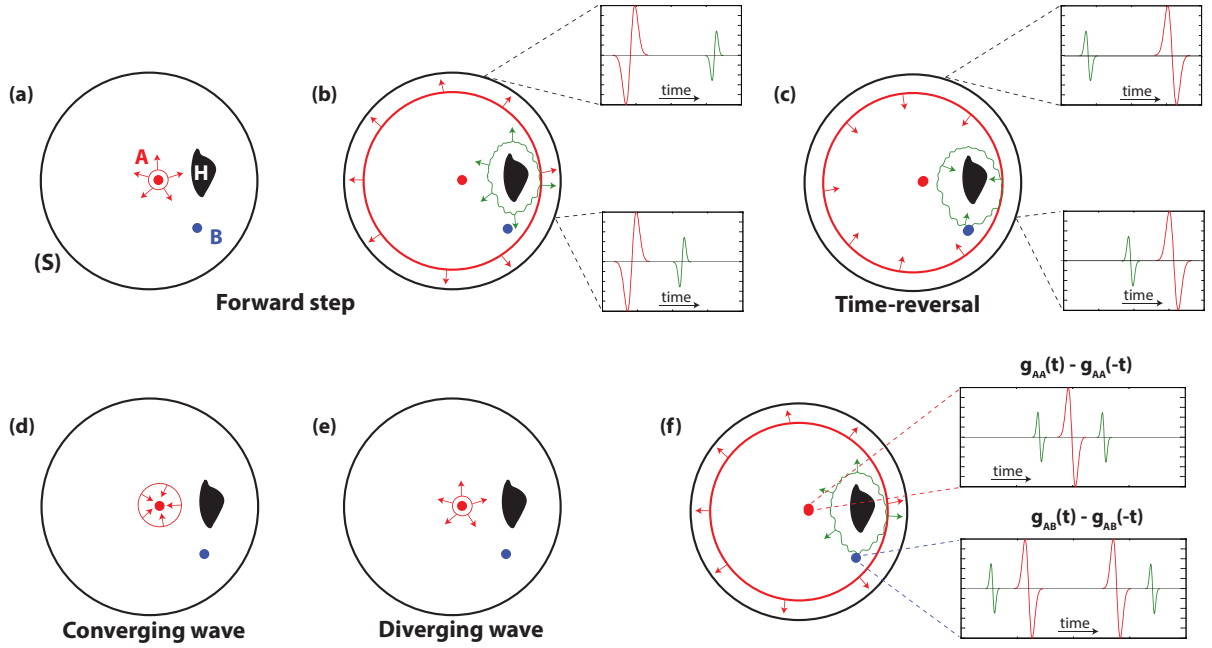


FIG. S1: Sketch of a TR experiment considering the example of a medium with a strong heterogeneity H (in black). (a) In a first step, a point source emits a pulse at position A . (b) The outgoing field is recorded by the TRM placed on the surrounding surface S . It contains both the direct wave-front (in red) and the wave-field scattered by H (in green). (c) In a second step, the TRM back-emits the time-reversed replica of the outgoing field. The time-reversed direct and scattered waves exactly follow the same trajectory as in the first step but in a reversed way. (d) Both waves finally converge at the same time towards the initial source position. (e) The converging wave collapses and is then followed by a diverging wave. (f) The fields measured at points A and B during the TR operation correspond exactly to the difference between the causal and anticausal Green's functions, $g_{AA}(t) - g_{AA}(-t)$ and $g_{AB}(t) - g_{AB}(-t)$, respectively. Both Green's functions g_{AA} and g_{AB} exhibit a direct component (in red) and a scattered component (in green) due to the presence of the heterogeneity H in the vicinity of points A and B .

$$\mathbf{E}_{\text{tr}}(\mathbf{r}, \omega) \cdot \mathbf{V} = \int_S \left[\overline{\mathbf{G}}^*(\mathbf{r}_s, \mathbf{r}_a, t) \mathbf{U}^* \times \nabla_{\mathbf{r}_s} \times \overline{\mathbf{G}}(\mathbf{r}, \mathbf{r}_s, \omega) \mathbf{V} - \overline{\mathbf{G}}(\mathbf{r}, \mathbf{r}_s, \omega) \mathbf{V} \times \nabla_{\mathbf{r}_s} \times \overline{\mathbf{G}}^*(\mathbf{r}_s, \mathbf{r}_a, \omega) \mathbf{U}^* \right] \cdot \mathbf{n} dS \quad (\text{S7})$$

If the time reversal mirror is located in the far field of the source and observation points, and if the medium close to the TRM is homogeneous, the vector form of the Sommerfeld's radiation condition [4, 5] can be used to write the curls of the retarded and advanced Green's functions as

$$\nabla_{\mathbf{r}_s} \times \overline{\mathbf{G}}(\mathbf{r}, \mathbf{r}_s, \omega) \simeq i\mathbf{k} \times \overline{\mathbf{G}}(\mathbf{r}, \mathbf{r}_s, \omega) \quad (\text{S8})$$

$$\nabla_{\mathbf{r}_s} \times \overline{\mathbf{G}}^*(\mathbf{r}_s, \mathbf{r}_a, \omega) \simeq -i\mathbf{k} \times \overline{\mathbf{G}}^*(\mathbf{r}_s, \mathbf{r}_a, \omega). \quad (\text{S9})$$

with $\mathbf{k} = k\mathbf{r}_s/r_s = k\mathbf{n}$. This approximation leads to the following expression for the time-reversed wave-field [Eq.S7]:

$$\mathbf{E}_{\text{tr}}(\mathbf{r}, \omega) \cdot \mathbf{V} = i \int_S \left[\overline{\mathbf{G}}^*(\mathbf{r}_s, \mathbf{r}_a, \omega) \mathbf{U}^* \times \left\{ \mathbf{k} \times \overline{\mathbf{G}}(\mathbf{r}, \mathbf{r}_s, \omega) \mathbf{V} \right\} + \overline{\mathbf{G}}(\mathbf{r}, \mathbf{r}_s, \omega) \mathbf{V} \times \left\{ \mathbf{k} \times \overline{\mathbf{G}}^*(\mathbf{r}_s, \mathbf{r}_a, \omega) \mathbf{U}^* \right\} \right] \cdot \mathbf{n} dS \quad (\text{S10})$$

One can develop the terms under the integral using the equality $\mathbf{x} \times (\mathbf{y} \times \mathbf{z}) = (\mathbf{x} \cdot \mathbf{z})\mathbf{y} - (\mathbf{x} \cdot \mathbf{y})\mathbf{z}$. As the wave vector \mathbf{k} is collinear to \mathbf{n} under the far-field approximation, as well as perpendicular to $\overline{\mathbf{G}}^*(\mathbf{r}_s, \mathbf{r}_a, t) \mathbf{U}^*$ and $\overline{\mathbf{G}}(\mathbf{r}, \mathbf{r}_s, \omega) \mathbf{V}$, the time-

reversed field can be finally expressed as,

$$\mathbf{E}_{\text{tr}}(\mathbf{r}, \omega) \cdot \mathbf{V} = 2ik \int_S dS \left[\overline{\mathbf{G}}(\mathbf{r}, \mathbf{r}_s, \omega) \mathbf{V} \right] \cdot \left[\overline{\mathbf{G}}^*(\mathbf{r}_s, \mathbf{r}_a, \omega) \mathbf{U}^* \right] \quad (\text{S11})$$

Due to spatial reciprocity, $\overline{\overline{\mathbf{G}}}(\mathbf{r}, \mathbf{r}_s, \omega) = \overline{\overline{\mathbf{G}}}^T(\mathbf{r}_s, \mathbf{r}, \omega)$, where the superscript T stands for transpose. Hence, Eq.S11 can be rewritten as

$$\mathbf{E}_{\text{tr}}(\mathbf{r}, \omega) \cdot \mathbf{V} = 2ik \int_S dS \left[\overline{\overline{\mathbf{G}}}^T(\mathbf{r}_s, \mathbf{r}, \omega) \overline{\overline{\mathbf{G}}}^*(\mathbf{r}_s, \mathbf{r}_a, \omega) \mathbf{U}^* \right] \cdot \mathbf{V} \quad (\text{S12})$$

The time reversed wave-field can be seen as a sum of cross-correlation of Green dyadics at the initial point source and the observation point. The comparison between the two expressions found for the time-reversed wave-field [Eq.S6 and Eq.S12] leads to the following equality

$$\begin{aligned} 2ik \int_S dS \overline{\overline{\mathbf{G}}}^T(\mathbf{r}_s, \mathbf{r}, \omega) \overline{\overline{\mathbf{G}}}^*(\mathbf{r}_s, \mathbf{r}_a, \omega) \\ = \overline{\overline{\mathbf{G}}}(\mathbf{r}, \mathbf{r}_a, \omega) - \overline{\overline{\mathbf{G}}}^*(\mathbf{r}, \mathbf{r}_a, \omega) \\ = 2i \text{Im} \left\{ \overline{\overline{\mathbf{G}}}(\mathbf{r}, \mathbf{r}_a, \omega) \right\} \end{aligned} \quad (\text{S13})$$

The last equality implies that, in the frequency domain, the spatial correlation of the field induced by the surface S at two points directly provides the imaginary part of the Green

dyadic connecting these two points. In the time domain, the latter quantity corresponds to the difference between the causal and anticausal Green dyadic [Eq.S5].

We now establish the link between TR and the correlation of a random wave-field. The perfect time reversal mirror is now replaced by a set of noise sources continuously distributed over the surface S [see Fig.S2]. The surface source distribution $\mathbf{N}(\mathbf{r}_s, \omega)$ is supposed to be perfectly incoherent, such that each of its component checks

$$\langle N_k(\mathbf{r}_s, \omega) N_l^*(\mathbf{r}'_s, \omega) \rangle = |\Gamma_\omega|^2 \delta_{kl} \delta(\mathbf{r}_s - \mathbf{r}'_s) \quad (\text{S14})$$

where the symbol $\langle \dots \rangle$ denotes an ensemble average and $|\Gamma_\omega|^2 = \langle |N_k(\mathbf{r}_s, \omega)|^2 \rangle$ is the power spectral density of noise. Such a source distribution generates an incoherent wave-field $\mathbf{E}(\mathbf{r}, t)$, which can be expressed as

$$\mathbf{E}(\mathbf{r}, \omega) = \int_S dS \overline{\overline{\mathbf{G}}}(\mathbf{r}, \mathbf{r}_s, \omega) \mathbf{N}(\mathbf{r}_s, \omega) \quad (\text{S15})$$

The associated correlation function $C(\mathbf{r}_a, \mathbf{r}_b, \omega)$ at two points \mathbf{r}_a and \mathbf{r}_b is thus given by

$$\begin{aligned} C(\mathbf{r}_a, \mathbf{r}_b, \omega) &= \langle \mathbf{E}(\mathbf{r}_a, \omega) \cdot \mathbf{E}^*(\mathbf{r}_b, \omega) \rangle = \left\langle \int_S \int_S dS dS' \left[\overline{\overline{\mathbf{G}}}(\mathbf{r}_a, \mathbf{r}_s, \omega) \mathbf{N}(\mathbf{r}_s, \omega) \right] \cdot \left[\overline{\overline{\mathbf{G}}}(\mathbf{r}_b, \mathbf{r}'_s, \omega) \mathbf{N}(\mathbf{r}'_s, \omega) \right]^* \right\rangle \quad (\text{S16}) \\ &= \int_S \int_S dS dS' \sum_{i,j,k} \overline{\overline{G}}_{ij}(\mathbf{r}_a, \mathbf{r}_s, \omega) \overline{\overline{G}}_{ik}^*(\mathbf{r}_b, \mathbf{r}'_s, \omega) \langle N_j(\mathbf{r}_s, \omega) N_k^*(\mathbf{r}'_s, \omega) \rangle \end{aligned}$$

The assumption of a perfectly incoherent noise source distribution [Eq.S14] allows to simplify the last expression,

$$\begin{aligned} C(\mathbf{r}_a, \mathbf{r}_b, \omega) &= \\ |\Gamma_\omega|^2 \int_S dS \sum_{i,j} \overline{\overline{G}}_{ij}(\mathbf{r}_a, \mathbf{r}_s, \omega) \overline{\overline{G}}_{ij}^*(\mathbf{r}_b, \mathbf{r}_s, \omega) \end{aligned} \quad (\text{S17})$$

The double sum in the last equation actually corresponds to the trace of the tensor $\overline{\overline{\mathbf{G}}}^T(\mathbf{r}_s, \mathbf{r}_a, \omega) \overline{\overline{\mathbf{G}}}^*(\mathbf{r}_s, \mathbf{r}_b, \omega)$, hence the following expression for the correlation of the incoherent wave-field

$$\begin{aligned} C(\mathbf{r}_a, \mathbf{r}_b, \omega) &= \\ |\Gamma_\omega|^2 \text{Tr} \left[\int_S dS \overline{\overline{\mathbf{G}}}^T(\mathbf{r}_s, \mathbf{r}_a, \omega) \overline{\overline{\mathbf{G}}}^*(\mathbf{r}_s, \mathbf{r}_b, \omega) \right] \end{aligned} \quad (\text{S18})$$

We here recognize the spatial correlation of the Green dyadic that appeared previously in the expression of the time-reversed wave-field [Eq.S12]. Hence, spatial correlation of a random wave-field and TR are mathematically equivalent. Hence, we can now establish the direct link between the time-dependent Green dyadic and the mutual coherence function $C(\mathbf{r}_a, \mathbf{r}_b, t)$ of a random wave-field. To that aim, we first in-

ject Eq.S13 into Eq.S18

$$i\omega C(\mathbf{r}_a, \mathbf{r}_b, \omega) = \frac{c}{2} |\Gamma_\omega|^2 \text{Tr} \left[\overline{\overline{\mathbf{G}}}(\mathbf{r}_b, \mathbf{r}_a, \omega) - \overline{\overline{\mathbf{G}}}^*(\mathbf{r}_b, \mathbf{r}_a, \omega) \right] \quad (\text{S19})$$

An inverse Fourier transform finally leads to the main result of this section, namely the proportionality between the time-derivative of the mutual coherence function $C(\mathbf{r}_a, \mathbf{r}_b, t)$ and the trace of the time-dependent Green dyadic $\overline{\overline{\mathbf{g}}}(\mathbf{r}, \mathbf{r}_a, t)$

$$\partial_t C(\mathbf{r}_a, \mathbf{r}_b, t) \propto \text{Tr} \left[\overline{\overline{\mathbf{g}}}(\mathbf{r}_b, \mathbf{r}_a, t) - \overline{\overline{\mathbf{g}}}(\mathbf{r}_b, \mathbf{r}_a, -t) \right] \otimes s(t) \quad (\text{S20})$$

with $s(t) = \gamma(t) \otimes \gamma(-t)$ is the inverse Fourier transform of the power spectral density $|\Gamma_\omega|^2$.

For the sake of simplicity, we refer to the trace of the Green dyadic as the Green's function in the accompanying Letter. Actually, in free space and in absence of source, the electromagnetic wave equation reduces to

$$\nabla^2 \mathbf{E}(\mathbf{r}, t) - \frac{1}{c^2} \frac{\partial^2 \mathbf{E}(\mathbf{r}, t)}{\partial t^2} = 0 \quad (\text{S21})$$

The free space Green dyadic $\overline{\overline{\mathbf{g}}}_0(\mathbf{r}_b, \mathbf{r}_a, t)$ is then simply given by

$$\overline{\overline{\mathbf{g}}}_0(\mathbf{r}_b, \mathbf{r}_a, t) = g_0(\mathbf{r}_b, \mathbf{r}_a, t) \overline{\overline{\mathbf{I}}} \quad (\text{S22})$$

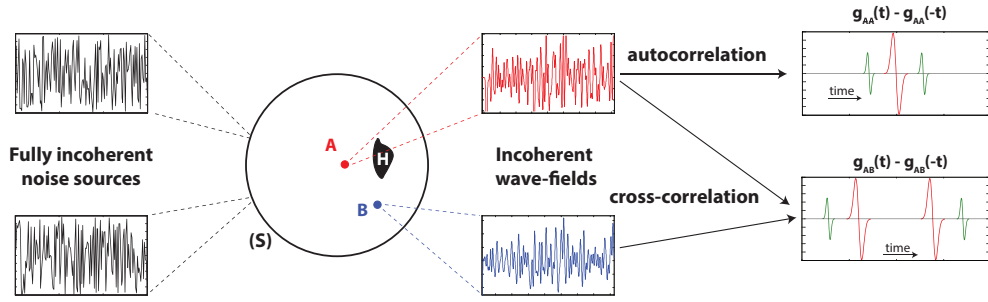


FIG. S2: Link between the mutual coherence of a random wave-field and the Green's function. A set of noise sources distributed over the surface S generates a perfectly incoherent wave-field. Although the field measured at point A seems to be noise-like, the time-derivative of its autocorrelation actually yields the difference between the causal and anticausal self Green's functions, $g_{AA}(t) - g_{AA}(-t)$. $g_{AA}(t)$ exhibits both a direct component at time $t = 0$ (in red) and a scattered component (in green) due to the presence of the strong heterogeneity H (in black) in the vicinity of A . Although the fields measured at points A and B seems to be *a priori* completely uncorrelated, the time-derivative of their cross-correlation actually yields the difference between the causal and anticausal Green's functions between A and B . $g_{AB}(t)$ exhibits both a direct component (in red) and a scattered component (in green). The comparison with the sketch of a TR experiment shown in Fig.S1 highlights the link between mutual coherence function of a random wave-field and TR.

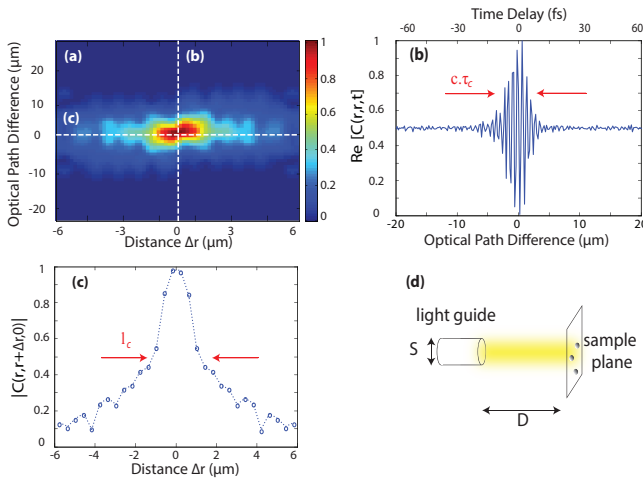


FIG. S3: (a) Space-time dependence of the interference pattern of the incident wave-field recorded with the Michelson interferometer. (b) Interference pattern vs OPD or time delay for zero mirror tilt. (c) Spatial dependence of the interference pattern at zero OPD obtained by tilting mirror M2 [see Fig.1 of the accompanying Letter]. (d) Physical parameters governing the coherence length of an incoherent wave-field according to the van-Citter Zernike theorem [Eq.S25].

with $g_0(\mathbf{r}_b, \mathbf{r}_a, t) = \delta(t - \|\mathbf{r}_b - \mathbf{r}_a\|/c)/(4\pi\|\mathbf{r}_b - \mathbf{r}_a\|)$ the Green's function of the scalar wave equation. Hence, in free space, the mutual coherence function C_0 [Eq.S20] is directly proportional to the difference between the causal and anticausal scalar Green's functions,

$$\partial_t C_0(\mathbf{r}_a, \mathbf{r}_b, t) \propto [g_0(\mathbf{r}_b, \mathbf{r}_a, t) - g_0(\mathbf{r}_b, \mathbf{r}_a, -t)] \otimes s(t) \quad (\text{S23})$$

TEMPORAL AND SPATIAL COHERENCE OF THE INCIDENT WAVE-FIELD

In this section, we investigate the spatial and temporal correlation of the incident wave-field which illuminates the scattering sample in the experiments described in the accompany-

ing Letter. This incident wave-field originates from a Halogen light source which isotropically illuminates the sample with three flexible light guides.

Fig.S3(a) displays the spatio-temporal interference pattern measured by the CCD camera. The time-dependence is controlled by the optical path difference (OPD) between the two interferometric arms. The temporal coherence τ_c of the incoherent light source is given by [6]

$$\tau_c \sim \frac{1}{\Delta f} = \frac{\lambda_c^2}{c\Delta\lambda} \quad (\text{S24})$$

with Δf the frequency bandwidth of the light source, $\lambda_c = 750$ nm its central wavelength and $\Delta\lambda = 200$ nm its spectral width. This yields a temporal coherence $\tau_c \sim 10$ fs which actually corresponds to the OPD range of $3 \mu\text{m}$ displayed by the interference pattern in Fig.S3(b).

Fig.S3(c) displays the spatial dependence of the interference pattern which is controlled by the tilt of mirror M2 as shown in Fig.1 of the accompanying Letter. Theoretically, the coherence length of the incident wave-field is given by the van-Citter Zernike theorem [6, 7]. It states that the coherence length should evolve as

$$l_c \sim \frac{\lambda_c D}{S} \quad (\text{S25})$$

where D is the distance between the output of the light guide and the scattering sample and S is the characteristic size of the guide section [see Fig.S3(d)]. Here $D = 40$ mm and $S = 10$ mm, hence l_c should be equal to $3 \mu\text{m}$ which is actually the spatial extent of the interference pattern measured experimentally [see Fig.S3(c)]. However, note that a residual spatial coherence subsists for points separated by more than l_c , as mentioned in the accompanying Letter.

* Electronic address: alexandre.aubry@espci.fr

[1] K. Wapenaar, E. Slob, and R. Snieder, Phys. Rev. Lett. **97**, 234301 (2006).

- [2] A. Derode, E. Larose, M. Tanter, M. Campillo, and M. Fink, J. Acoust. Soc. Am. **113**, 2973 (2003).
- [3] M. Fink, J. Physics: Conference Series **124**, 012004 (2008).
- [4] R. Carminati, R. Pierrat, J. de Rosny, and M. Fink, Opt. Lett. **32**, 3107 (2007).
- [5] M. Nieto-Vesperinas, Scattering and Diffraction in Physical Optics, 2nd ed. (World Scientific Publishing Co. Pte. Ltd., Singapore, 2006).
- [6] J. Goodman, Statistical Optics: An Introduction (Wiley, New York, 1984).
- [7] F. Zernike, Physica **5**, 785 (1938).